

Numerical simulations of pressures applied on a cylindrical silo with hopper due to a granular material by using FEM and DEM

Sami Houhamdi*, Eutiquio Gallego Vazquez**, Kamel Djeghaba*

* Civil engineering laboratory, University of Badji Mokhtar - Annaba, Algeria

** Department of Agricultural Engineering, BIPREE Research Group, ETSI Agronomica, Alimentaria y de Biosistemas, Universidad Politecnica de Madrid, 28040 Madrid, Spain

Article Info

Article history:

Received###/###/#####

Revised ###/###/#####

Accepted ###/###/#####

Keyword:

FEM simulation, DEM simulation, Granular material, Steel silo, Hopper

Corresponding Author:

Sami Houhamdi,

Civil engineering laboratory, University of Badji Mokhtar - Annaba, PB 12, Annaba, Algeria

Email: sami.houhamdi@univ-annaba.org; sami.houhamdi@gmail.com

ABSTRACT

In this work, we have simulated the behavior of the granular flow of dry wheat material inside a cylindrical steel silo with a concentric hopper during the filling and emptying process. The influence on the wall was studied by obtaining the pressures and stresses using the Finite Element Method (MEF) and Discrete Element Method (DEM). The obtained results by the analytical formulas of EUROCODE, the FEM and DEM are compared. The analyzed results include the vertical distributions of pressures that the ensiled material exerted on the silo walls and the distributions of normal and tangential stresses under extreme actions of emptying and filling. The results show that the DEM simulation is more realistic even by using the upscaling technique with a particle scale factor of 10. The pressures obtained by simulations are close to those obtained by EC, and the stresses are almost identical.

1. INTRODUCTION

Silos are widely used structures for stored materials, especially agriculture [1]. Owing to its importance, durability and safety have to be ensured by obtaining the correct dimensions, which are calculated based on the action and forces applied on the walls of the silo. The European standard of Eurocode[2] is widely used to determine the applied actions on the silo walls, and its formulas are based on analytical approaches ([3], [4]). For more understanding of the bulk material behavior inside silos, many experiments have been performed ([5]–[8]). However, some problems remain unresolved ([9], [10]). Another approach to evaluate the applied forces is the numerical simulation, where recently, with the development of computer capabilities, numerical simulation of silos is widely spread. Basically, there are two main numerical methods to perform a simulation of silos, the first is the Finite Element Method (FEM) [11], and the second is the Discrete Element Method (DEM) [12].

For many years, the FEM was the most used tool to simulate the filling and emptying of silos ([13]–[17]), and that is because of the limited capabilities of computers during the first spread period of the numerical methods. FEM calculation is simple enough to perform by using the old computers, especially with some simplifications, such as reducing the mesh size and performing static linear analysis. FEM simulations have been performed by many researchers with results close to experimental tests (specifically the pressures applied on the silo walls) [14]. However, this method is not able enough to simulate all particles behavior, such as the mass flow and particle's velocity. In addition, it is just a simplified procedure that is based on modeling the particles as one solid object that occupies the volume inside the silo ([17], [18]), which is not the real case of the ensiled material, where every individual particle is separated and has its own velocity and path. Furthermore, there are many difficulties in solving the nonlinear problem with convergence results in the case of complicated parameters and advanced element types.

Recently, the DEM is the most widely used technique to simulate the granular flow due to its accuracy of behavior predicting and the obtained realistic results ([19]–[25]). The discharge rate ([26], [27]), segregation ([28], [29]), flow pattern ([30]–[32]), and the pressure distribution ([33]–[37]) are some of the most features that are studied by DEM. However, the inconvenience of this method is the computational time which can take days or even weeks to perform the simulation. Unlike the FEM, DEM is based on creating a model of the individual grain, and in the simulation process, multiple particles are generating to simulate the granular flow. The contact between the particles is determined during the simulation and a new direction and velocity are assigned to every particle based on the amount of contact overlap. This process is repeated every time step, which is calculated as a fraction of Rayleigh's time step criterion [38] and the normal range is between 10% and 40% of Rayleigh's time. "Upscaling" technique or "Coarse-Graining" is a common method that is usually used to reduce particles number leading to reduce the computing time ([39]–[45]). It is based on scaling the size of the particle to represent a

group of particles. This technique has been studied by many authors, see for example([46]–[48]), where they found that it is possible to get an accurate prediction of results.

The present work analyses the numerical results obtained by using FEM and DEM models of a cylindrical steel silo with a concentric hopper during the filling and discharging by using wheat material. The vertical distributions of normal and tangential pressures on the silo walls, as well as the circumferential and longitudinal stresses, were all studied. The numerical results obtained for the two methods were compared with the analytical method of Eurocode. The discrete element method is a good technique for obtaining a great simulation and dealing with real case problems. Unfortunately, its disadvantage is caused by the computational time consuming compared to the FEM.

2. RESEARCH METHOD

In this work, we have performed two different simulations. The first is based on the finite element method, and the second is on the discrete element method. The same silo geometry has been used in both simulations but with a different bulk material model. In the FEM, we have considered the entire bulk material as a solid object with appropriate nonlinear material properties, while the DEM uses a real particle shape based on the multi-sphere method with the material properties of each individual grain. The bulk density behavior was simulated by generating a huge number of particles to fill the silo.

2.1. Silo dimensions

The used silo in the simulations is designed by a research team at the Agricultural Engineering and Sciences Department, University of León, Spain. Its geometry is divided into two parts of steel walls with a 3 mm thickness. The first is the vertical silo wall of 2 m height and 1 m in diameter. The second part is the hopper, which has a 0.48 m height and an outlet with a 0.35 m diameter, see Figure 1[6], [7], [14].

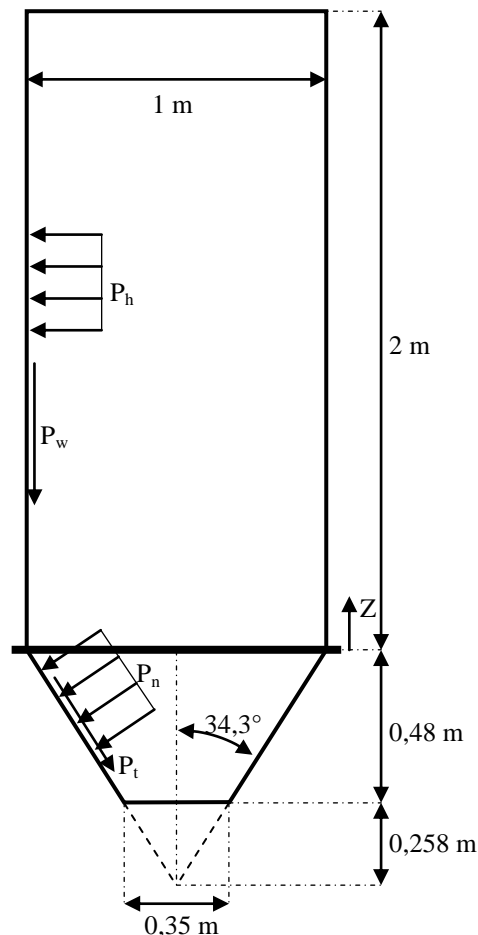


Figure 1. The dimensions and design of the used silo for both simulations.

2.2. Finite Element model

The FEM model of the steel silo and the stored material are completely simulated with the software “ANSYS Workbench v17.2”.

2.2.1. Bulk material model

The granular material used to evaluate the exerting loads on the silo walls due to the stored material is the dry wheat, with mechanical properties shown in Table 1. These characteristics are determined at the School of Agricultural Engineering of the University of Leon, which contains: the density of the bulk material ρ_b ,

modulus of elasticity of the bulk E_b , the angle of internal friction of the stored material φ_b , the coefficient of friction on the wall μ_b and Poisson's ratio of the bulk ν_b , which has been deduced from the pressure ratio K_b using Equation (1) ([5], [14]).

$$\nu = \frac{K}{1 + K} \quad (1)$$

The other parameters such as the cohesion C_b , the angle of dilation ψ_b , the density of the steel ρ_s , the modulus of elasticity of the steel E_s , the Poisson's ratio of the steel ν_s , were adopted from the literature as shown in Table 1.

Table 1. Characteristics of the bulk material and the steel silo.

	The property	The value
The characteristics of the stored material:	The density ρ_b (kN / m ³)	8.397
	Modulus of elasticity E_b (kPa)	10674
	Cohesion C_b (kPa)	2
	Internal friction angle φ_b (degree)	30.17°
	The angle of dilatancy ψ_b (degree)	8.0°
	Pressure ratio $K_{b,f}$ (Filling)	0.333
	Pressure ratio $K_{b,e}$ (Emptying)	0.724
	Poisson's ratio $\nu_{b,f}$ (Filling)	0.25
	Poisson's ratio $\nu_{b,e}$ (Emptying)	0.42
The characteristics of steel:	The density ρ_s (kN / m ³)	78.6
	Modulus of elasticity E_s (kPa)	2.1×10^8
	Poisson's ratio ν_s	0.3
	Coefficient of friction on the wall μ	0.2

2.2.2. Mesh element type

The element type *SOLID45* is used for the 3D mesh of the stored material, which is defined by 8 nodes having three degrees of freedom at each node (translations in the nodal directions x, y, and z). The *SHELL281* element was used to model the silo wall, which has 8 nodes with 6 degrees of freedom at each node (translations in the x, y, and z axes, and rotations around the x, y, and z).

2.2.3. Contact type

The simulation of the contact between the silo walls and the bulk material is performed with the most helpful type for this case, namely "no separation". The Coulomb friction model was used to define the interaction between the silo wall and the stored material. The friction coefficient between the wall and the stored material is the only required parameter to simulate this interaction. To avoid certain convergence problems, a distance of 0.1 mm has been taken into account between the silo wall and the stored material. The friction coefficient is introduced with the APDL command.

2.2.4. Boundary conditions

To calculate the pressure on the silo, according to the Eurocode classification, the walls are assumed to be rigid, the reason why all movements of the nodes simulating the silo wall have been blocked. In the stress analysis, only the vertical displacement of the nodes placed on the transition was blocked. Some additional blockings were required, the displacements of the nodes of the stored material located in the outlet were blocked for the filling analysis. This blockage was deleted when the discharge began. The only load taken into account in the analysis is the total weight of the stored material, the density of which is (8.397 kN/m³).

2.2.5. Material model

The behavior of the steel wall was represented by an isotropic elastic linear model. No plasticity was considered for the steel wall since the expected stresses are very far from the elastic limit. Only two parameters are necessary to define the behavior of the steel wall: the Poisson's ratio ν_s and the modulus of elasticity E_s .

The model of the stored material was simulated with an elastoplastic behavior law. The elastic part was represented by an isotropic linear model, using the material parameters: the modulus of elasticity E_b and the Poisson's ratio ν_b . In contrast, the plastic part was defined by the perfectly plastic criterion of Drucker-Prager with its three necessary parameters: the internal friction angle φ_b , the cohesion C_b , and the dilatancy angle ψ_b [14]. The classic Drucker-Prager model is assigned to the stored material with an APDL command.

2.2.6. Simulation process

The simulation of the gradual filling of a silo can be carried out with two possible approaches. The first is to apply all the material at each moment, and its density gradually increases. The second approach consists of creating several layers of matter with their complete density ρ_b , and at each moment, one layer is activated until the last layer. The second approach is called "layer by layer", it was used to simulate the filling in this work using the "Birth and Death" function in ANSYS (Figure 2). The analysis is considered static in the case of filling (the influence of speeds and accelerations can be neglected). The "Newmark" method was used for the dynamic analysis of the emptying.

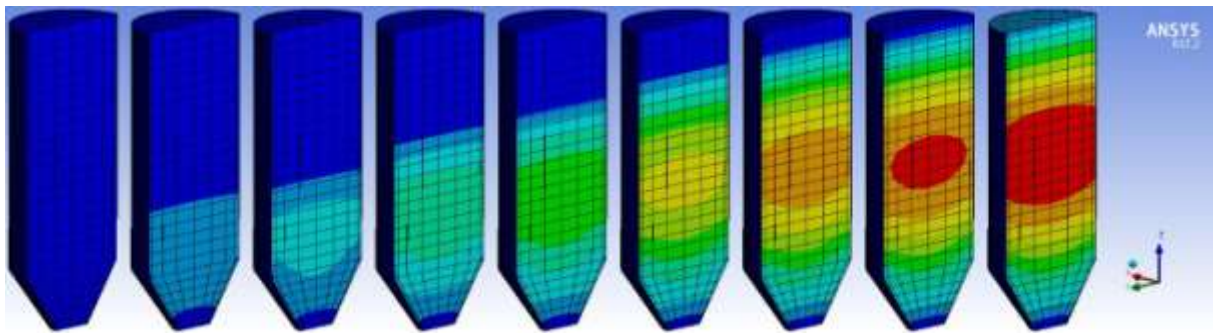


Figure 2. Bulk material deformation shows the gradual filling of the silo with the “layer by layer” approach.

2.3. Discrete Element model

2.3.1. Particle model

The particle model has been obtained from [49], where the clump of three spheres is used. The radii of every sphere are 1.25 mm, 1.5 mm, and 1.25 mm respectively, as shown in Figure 3. The distance between the centers of the spheres on the edges was 1.5 mm (Figure 3).

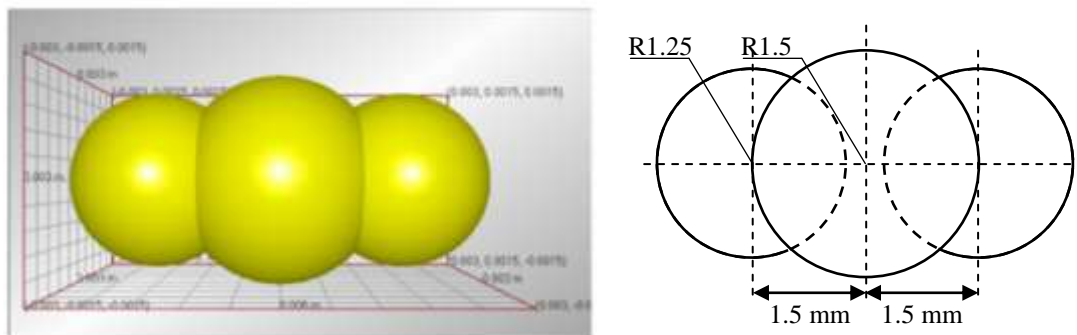


Figure 3. Particle model of the wheat grain.

All mechanical parameters of wheat particles used in DEM simulation are indicated in Table 2. The particle has Poisson’s coefficient ν_p of 0.4, the density ρ_p of 1430 kg/m³, and the shear modulus $G_p = 5.58 \times 10^8$ Pa. Silo walls are made of steel with the same parameters as the finite element model. Hertz-Mindlin no-slip contact model was used to model the interaction of wheat and silo walls where three parameters are needed, the static friction coefficient μ_0 , restitution coefficient G_r , and the rolling friction coefficient f , see Table 2[50].

Table 2. Mechanical parameters of the wheat particle.

Parameter	Value
Poisson’s ratio ν_p	0.4
Density ρ_p (kg/m ³)	1430
Shear modulus G_p (Pa)	3.58×10^8
Coefficient of restitution G_r	Wheat-Wheat: 0.5 Wheat-Steel: 0.6
Coefficient of static friction μ_0	Wheat-Wheat: 0.3 Wheat-Steel: 0.25
Coefficient of rolling friction f	Wheat-Wheat: 0.01 Wheat-Steel: 0.01

2.3.2. Simulation process

The DEM model was simulated by using EDEM Academic software [51]. The first step in the simulation was filling the silo with particles where a cylindrical generator was used to randomly generate particles at the top of the silo without any initial velocity. These particles were allowed to fall under gravity force to fill the entire silo progressively. The generator is deleted when the silo is completely filled. The wall closing the hopper outlet was removed, allowing the discharge simulation to proceed after particles reached the static state where the kinetic energy is almost null (Figure 4). We used 30% of Rayleigh’s time as a time step for this simulation. Due to the relatively large silo size, the simulation process could take a very long time. We used the upscaling technique with a particle radius scale factor of 10 to generate fewer particles number and to speed up the simulation.

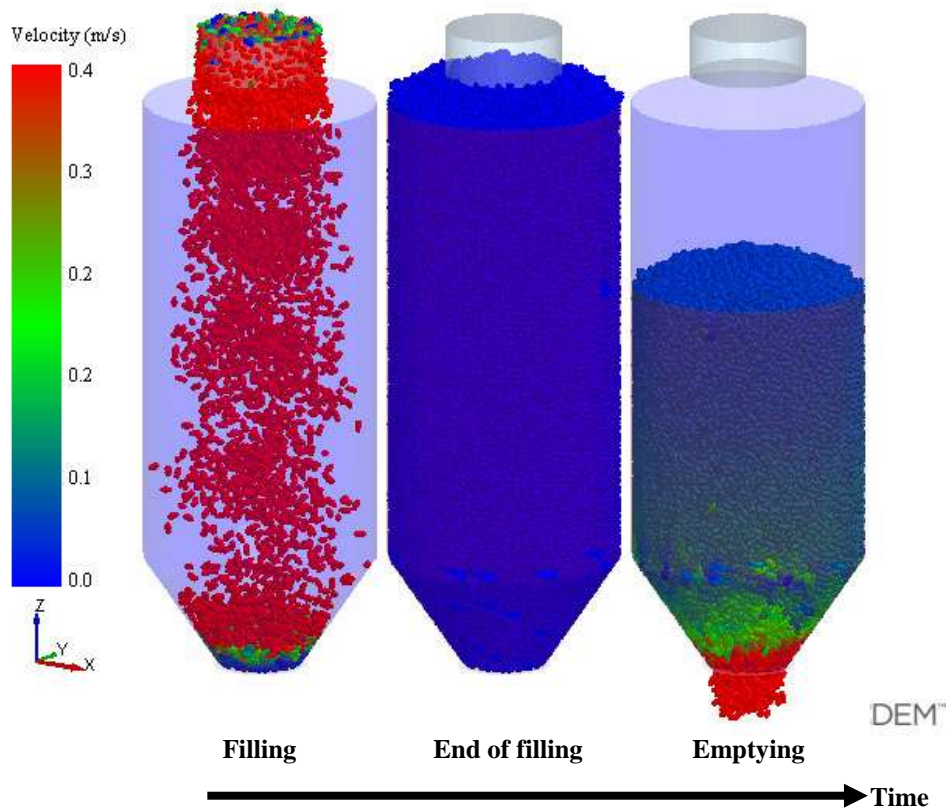


Figure 4. Simulation process of the filling and emptying of the virtual silo.

3. RESULTS AND DISCUSSION

3.1. Pressures

Figure 5 shows the values of the normal pressures calculated by Eurocode 1 part 4 and those obtained by both simulations FEM and DEM for both cases: filling and emptying. In the filling case, the pressures obtained by FEM are slightly lower than the EC, unlike the DEM pressures, which are slightly higher than those obtained by Eurocode along the vertical wall, except for the lower part where the two curves are almost the same. A slight reduction of DEM pressure can be seen at the bottom of the vertical wall, where it is equal to 3.6 kPa; however, the pressure evaluated by EC is 5.4 kPa. For FEM pressure, this reduction is more significant, and it has a negative value (-6.6 kPa). This is a typical trend that has been observed experimentally [52] and numerically ([53]–[55]). It is effectively caused by the material behavior at this point and the contact type for the FEM model. The compression force applied from the bin particles on the inclined hopper particles, makes the material deformed to the inner side at the point where the bin meets the hopper. The contact type “No

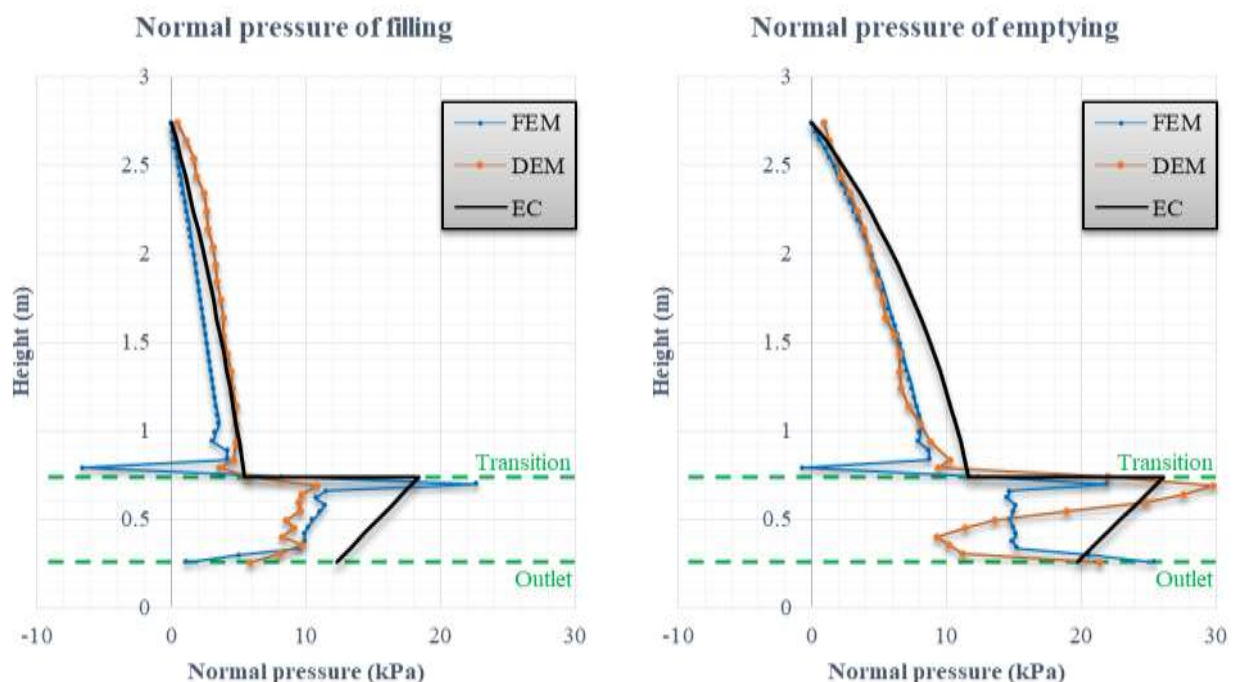


Figure 5. The values of the normal pressures in the silo walls due to filling and emptying by the FEM, DEM, and EC.

separation” prevents the material and the wall from separating, leading to a negative pressure value. The DEM model is different, i.e., the particles can separate freely from the walls so that the pressures are just reduced without a negative value. For the transition area, the pressure experienced a peak value (18.4 kPa for EC, 22.7 kPa for FEM, and 10.8 kPa for DEM), as widely observed by [7], [14], [52], [56], and it starts reducing over the hopper wall gradually. The leading cause of this tendency is the sudden change of particle direction from the vertical to the hopper inclination angle [57]. The peak value obtained by FEM is greater than that obtained by EC or DEM. Besides, unlike the vertical walls, the pressures of FEM are slightly greater than the DEM’s case along the hopper walls. On the other hand, the pressure obtained by EC is high compared to those calculated by FEM and DEM along the hopper walls.

The emptying case has greater values than the filling [52], and the pressures of FEM and DEM are almost the same along the vertical walls, except at the bottom of the bin walls where the same behavior appears as the filling case. The peak value of DEM is greater than the FEM at the transition zone. Nevertheless, the pressures obtained by FEM are greater along the lower part of the hopper. EC for the emptying case has greater values than both FEM and DEM results except the peak value of the transition zone, where the DEM pressures are more significant.

The tangential pressures obtained by FEM, DEM, and Eurocode are shown in Figure 6 for filling and emptying cases. DEM and EC values are roughly equal for the vertical wall, while the EC has greater values along with the hopper. However, the hopper experienced a higher DEM peak value than EC at the transition zone of the emptying case (11.8 kPa for DEM and 5.1 kPa for EC). FEM pressures are lower than both EC and DEM pressures for both the filling and emptying cases.

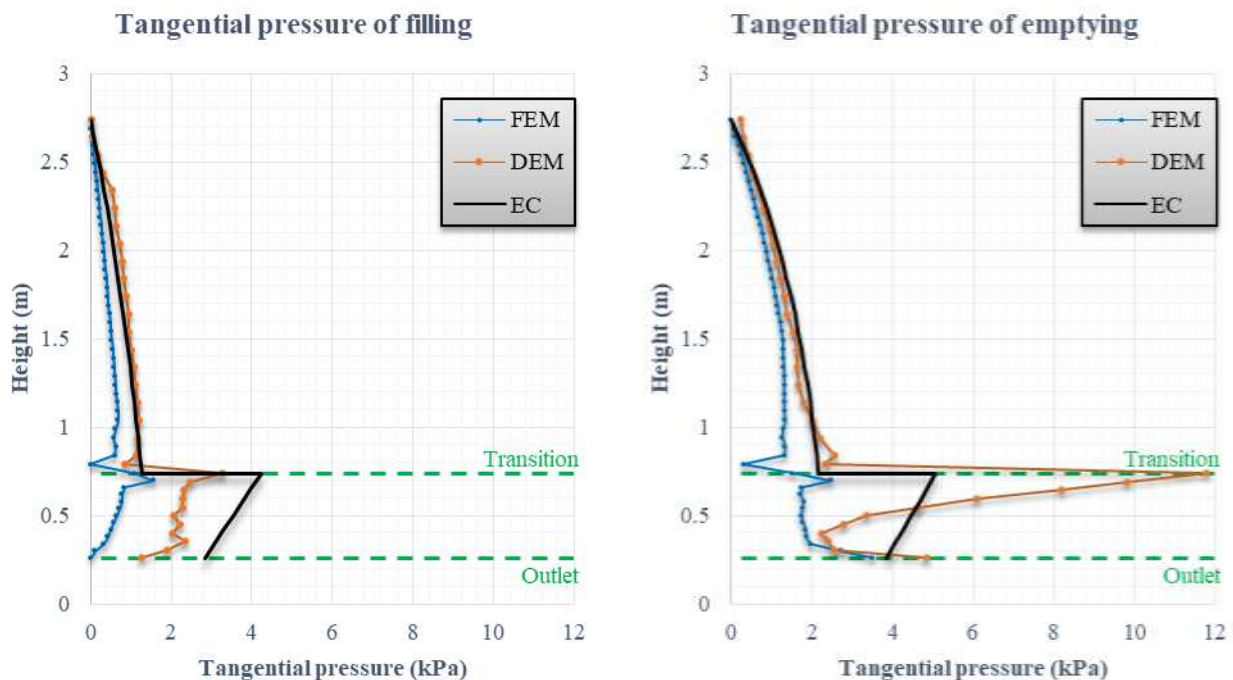


Figure 6. The values of the tangential pressures in the silo walls due to filling and emptying by the FEM, DEM, and EC.

3.2. Stresses

For the circumferential stresses s_{XX} (Figure 7), the results obtained by FEM and DEM are almost identical for both filling and emptying, except for the hopper walls of the emptying case, where DEM values are more significant. EC values are very close to the simulations of the filling case, particularly in the vertical wall of the silo. For the emptying case, the results of EC are slightly greater than both simulations at both walls, the vertical wall, and the hopper except at the transition area, where the peak value of DEM is greater than the EC one.

Longitudinal stresses s_{YY} are shown in Figure 8, representing the FEM, DEM, and EC results in the case of filling and emptying. The stress curve has negative values at the bin walls and positive values at the hopper. This returns to the blocked nodes at the transition zone, where the bin part is under compression and the hopper is under traction. The s_{YY} results of DEM are greater than FEM for both cases and the EC values are between the FEM and DEM values at the bin, while at the hopper the EC values are greater than both simulations.

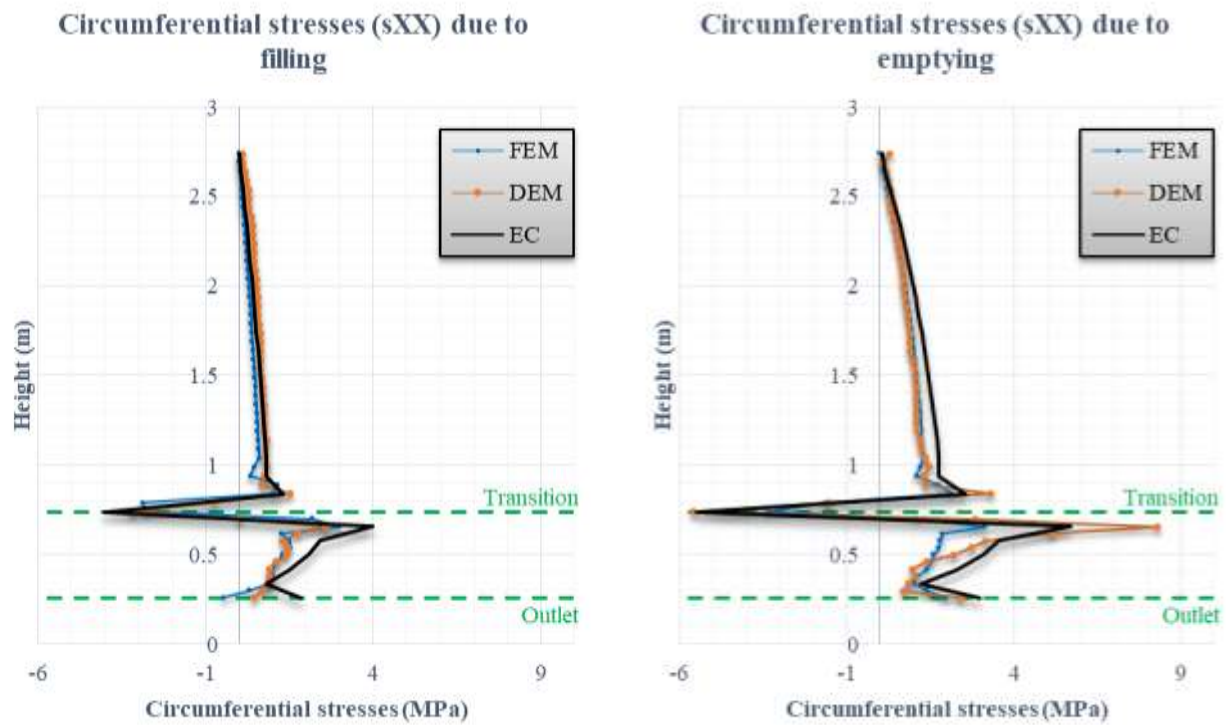


Figure 7. The values of the circumferential stresses in the silo walls due to filling and emptying by the FEM, DEM, and EC.

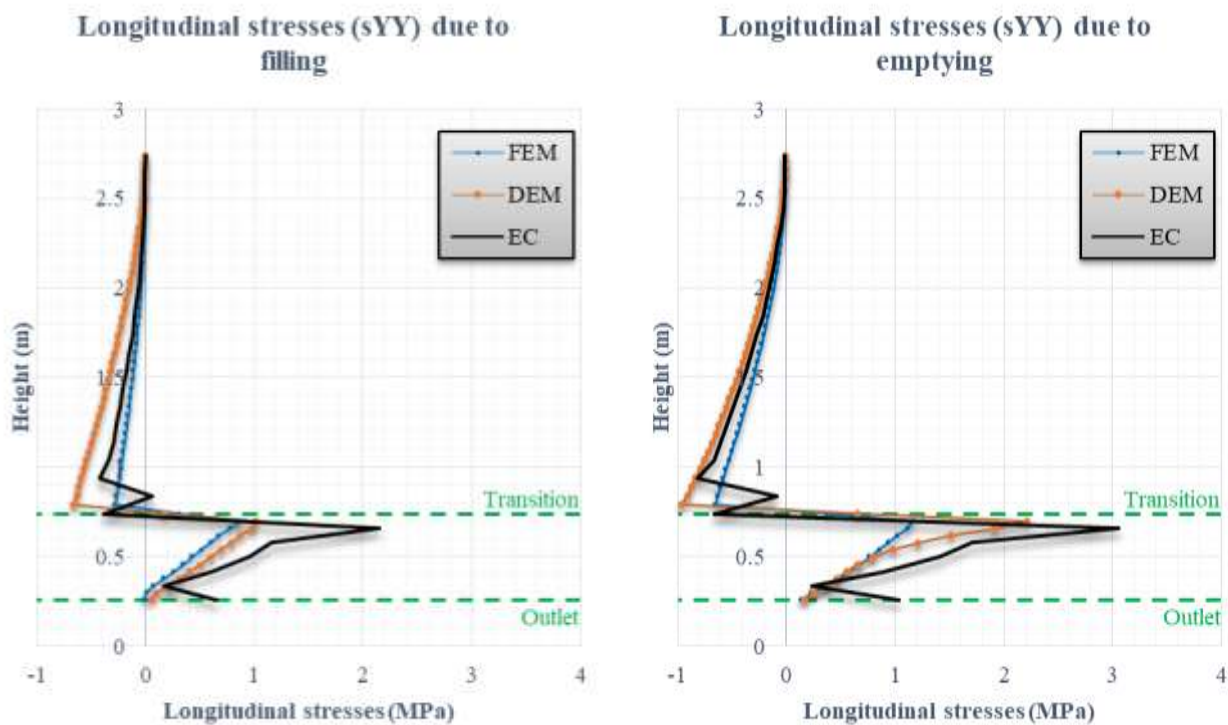


Figure 8. The values of the longitudinal stresses in the silo walls due to filling and emptying by the FEM, DEM, and EC.

4. CONCLUSION

The aim of this work is to simulate numerically the filling and the emptying of a steel silo with a concentric hopper by using two methods, the finite element and the discrete element methods, where the obtained results are essentially the pressures and stresses. A comparison between these two numerical methods and the analytical method of Eurocode is presented.

According to the results obtained by the numerical simulations of the silo during filling and emptying, it can be seen that the obtained pressures are close to those calculated by the Eurocode for both cases.

The hopper experienced a reduction of pressure values with DEM. However, the transition peak values have high values due to the emptying case compared to EC.

The values obtained by DEM simulation are greater than those obtained by FEM for the pressures and the stresses.

By comparing the numerical simulation (DEM) with the analytical method (Eurocode), we can notice that the obtained circumferential and longitudinal stresses are almost the same for the two studied cases.

FEM has remarkably lower tangential pressure and stress values than the EC and DEM simulations.

DEM simulation has the ability to simulate the complex behavior of the granular flow better than FEM, and even more, we can see clearly that at the bottom of the vertical walls, the FEM gives an unrealistic negative pressure.

Even using the upscaling technique with a scale factor of 10, the DEM results are still more accurate than the FEM simulation.

These results show the power of the discrete element method to simulate the granular material inside the silo for both filling and emptying. This capability allows us to easily manipulate the simulation of material behavior and deduce that we can apply it for more specific and complex silo problems.

REFERENCES

- [1] P. A. Langston, U. Tüzün, and D. M. Heyes, "Discrete element simulation of granular flow in 2D and 3D hoppers: Dependence of discharge rate and wall stress on particle interactions," *Chemical Engineering Science*, vol. 50, no. 6, pp. 967–987, Mar. 1995, doi: 10.1016/0009-2509(94)00467-6.
- [2] EN 1991-4, *Eurocode 1: Actions on Structures - Part 4: Silos and Tanks*. Brussels: CEN, 2006.
- [3] H. A. Janssen, "Versuch über Getreidedruck in Silozellen," *Zeitschrift des Vereins Deutscher Ingenieure*, vol. 39, pp. 1045–1049, 1895.
- [4] M. L. Reimbert and A. M. Reimbert, *Silos : Trait e th eorique et pratique*. Paris: Eyrolles, 1956.
- [5] A. Couto, A. Ruiz, and P. J. Aguado, "Experimental study of the pressures exerted by wheat stored in slender cylindrical silos, varying the flow rate of material during discharge. Comparison with Eurocode 1 part 4," *Powder Technology*, vol. 237, pp. 450–467, Mar. 2013, doi: 10.1016/j.powtec.2012.12.030.
- [6] A. Couto, A. Ruiz, and P. J. Aguado, "Design and instrumentation of a mid-size test station for measuring static and dynamic pressures in silos under different conditions – Part I: Description," *Computers and Electronics in Agriculture*, vol. 85, pp. 164–173, Jul. 2012, doi: 10.1016/j.compag.2012.04.009.
- [7] A. Ruiz, A. Couto, and P. J. Aguado, "Design and instrumentation of a mid-size test station for measuring static and dynamic pressures in silos under different conditions – Part II: Construction and validation," *Computers and Electronics in Agriculture*, vol. 85, pp. 174–187, Jul. 2012, doi: 10.1016/j.compag.2012.04.008.
- [8] P. Wang, L. Zhu, and X. Zhu, "Flow pattern and normal pressure distribution in flat bottom silo discharged using wall outlet," *Powder Technology*, vol. 295, pp. 104–114, Jul. 2016, doi: 10.1016/j.powtec.2016.03.036.
- [9] F. Ayuga, "Some unresolved problems in the design of steel cylindrical silos," in *Structures and Granular Solids: From Scientific Principles to Engineering Application*, CRC Press, 2008, pp. 123–133. doi: 10.1201/9780203884447.ch12.
- [10] J. Nielsen, "From silo phenomena to load models," in *Structures and Granular Solids: From Scientific Principles to Engineering Application*, CRC Press, 2008, pp. 49–57. doi: 10.1201/9780203884447.ch4.
- [11] O. C. Zienkiewicz and R. L. Taylor, *The Finite Element Method Set*. Elsevier, 2005.
- [12] P. A. Cundall and O. D. L. Strack, "A discrete numerical model for granular assemblies," *G eotechnique*, vol. 29, no. 1, pp. 47–65, Mar. 1979, doi: 10.1680/geot.1979.29.1.47.
- [13] J. Eibl, H. Landahl, U. Haeussler, and W. Gladen, "Problem of Stresses in Silo Structures," *Beton- Und Stahlbetonbau*, 1982.
- [14] E. Gallego, A. Ruiz, and P. J. Aguado, "Simulation of silo filling and discharge using ANSYS and comparison with experimental data," *Computers and Electronics in Agriculture*, vol. 118, pp. 281–289, Oct. 2015, doi: 10.1016/j.compag.2015.09.014.
- [15] Q. Meng, J. C. Jofriet, and S. C. Negi, "Finite Element Analysis of Bulk Solids Flow: Part 1, Development of a Model Based on a Secant Constitutive Relationship," *Journal of Agricultural Engineering Research*, vol. 67, no. 2, pp. 141–150, Jun. 1997, doi: 10.1006/jaer.1997.0161.
- [16] J. Y. Ooi and J. M. Rotter, "Wall pressures in squat steel silos from simple finite element analysis," *Computers and Structures*, vol. 37, pp. 361–374, 1990.
- [17] P. Vidal, E. Gallego, M. Guaita, and F. Ayuga, "Simulation of the Filling Pressures of Cylindrical Steel Silos with Concentric and Eccentric Hoppers Using 3-Dimensional Finite Element Models," *Transactions of the ASABE*, vol. 49, no. 6, pp. 1881–1895, 2006, doi: 10.13031/2013.22290.
- [18] P. Vidal, E. Gallego, M. Guaita, and F. Ayuga, "Finite element analysis under different boundary conditions of the filling of cylindrical steel silos having an eccentric hopper," *Journal of Constructional Steel Research*, vol. 64, no. 4, pp. 480–492, Apr. 2008, doi: 10.1016/j.jcsr.2007.08.005.
- [19] E. Gallego, J. M. Fuentes, J. Wi acek, J. R. Villar, and F. Ayuga, "DEM analysis of the flow and friction of spherical particles in steel silos with corrugated walls," *Powder Technology*, vol. 355, pp. 425–437, Oct. 2019, doi: 10.1016/j.powtec.2019.07.072.
- [20] S. Golshan, B. Esgandari, R. Zarghami, B. Blais, and K. Saleh, "Experimental and DEM studies of velocity profiles and residence time distribution of non-spherical particles in silos," *Powder Technology*, vol. 373, pp. 510–521, Aug. 2020, doi: 10.1016/j.powtec.2020.06.093.

- [21] J. Hlosta, L. Jezerská, J. Rozbroj, D. Žurovec, J. Nečas, and J. Zegzulka, “DEM Investigation of the Influence of Particulate Properties and Operating Conditions on the Mixing Process in Rotary Drums: Part I—Determination of the DEM Parameters and Calibration Process,” *Processes*, vol. 8, no. 2, p. 222, Feb. 2020, doi: 10.3390/pr8020222.
- [22] R. Kumar, C. M. Patel, A. K. Jana, and S. R. Gopireddy, “Prediction of hopper discharge rate using combined discrete element method and artificial neural network,” *Advanced Powder Technology*, vol. 29, no. 11, pp. 2822–2834, Nov. 2018, doi: 10.1016/j.apt.2018.08.002.
- [23] M. A. Najafi-Sani and Z. Mansourpour, “Application of a new method for experimental validation of polydispersed DEM simulation of silo discharge,” *Advanced Powder Technology*, vol. 31, no. 11, pp. 4457–4469, Nov. 2020, doi: 10.1016/j.apt.2020.09.021.
- [24] X. Wang, J. Yu, F. Lv, Y. Wang, and H. Fu, “A multi-sphere based modelling method for maize grain assemblies,” *Advanced Powder Technology*, vol. 28, no. 2, pp. 584–595, Feb. 2017, doi: 10.1016/j.apt.2016.10.027.
- [25] Y. Wang and J. Y. Ooi, “A Study of Granular Flow in a Conical Hopper Discharge Using Discrete and Continuum Approach,” *Procedia Engineering*, vol. 102, pp. 765–772, 2015, doi: 10.1016/j.proeng.2015.01.183.
- [26] A. Anand, J. S. Curtis, C. R. Wassgren, B. C. Hancock, and W. R. Ketterhagen, “Predicting discharge dynamics from a rectangular hopper using the discrete element method (DEM),” *Chemical Engineering Science*, vol. 63, no. 24, pp. 5821–5830, Dec. 2008, doi: 10.1016/j.ces.2008.08.015.
- [27] C. González-Montellano, Á. Ramírez, E. Gallego, and F. Ayuga, “Validation and experimental calibration of 3D discrete element models for the simulation of the discharge flow in silos,” *Chemical Engineering Science*, vol. 66, no. 21, pp. 5116–5126, Nov. 2011, doi: 10.1016/j.ces.2011.07.009.
- [28] W. R. Ketterhagen, J. S. Curtis, C. R. Wassgren, A. Kong, P. J. Narayan, and B. C. Hancock, “Granular segregation in discharging cylindrical hoppers: A discrete element and experimental study,” *Chemical Engineering Science*, vol. 62, no. 22, pp. 6423–6439, Nov. 2007, doi: 10.1016/j.ces.2007.07.052.
- [29] H. Xiao *et al.*, “Continuum modeling of granular segregation during hopper discharge,” *Chemical Engineering Science*, vol. 193, pp. 188–204, Jan. 2019, doi: 10.1016/j.ces.2018.08.039.
- [30] P. W. Cleary and M. L. Sawley, “DEM modelling of industrial granular flows: 3D case studies and the effect of particle shape on hopper discharge,” *Applied Mathematical Modelling*, vol. 26, no. 2, pp. 89–111, Feb. 2002, doi: 10.1016/S0307-904X(01)00050-6.
- [31] C. González-Montellano, F. Ayuga, and J. Y. Ooi, “Discrete element modelling of grain flow in a planar silo: influence of simulation parameters,” *Granular Matter*, vol. 13, no. 2, pp. 149–158, Apr. 2011, doi: 10.1007/s10035-010-0204-9.
- [32] T. Tian, J. Su, J. Zhan, S. Geng, G. Xu, and X. Liu, “Discrete and continuum modeling of granular flow in silo discharge,” *Particuology*, vol. 36, pp. 127–138, Feb. 2018, doi: 10.1016/j.partic.2017.04.001.
- [33] R. Balevičius, I. Sielamowicz, Z. Mróz, and R. Kačianauskas, “Investigation of wall stress and outflow rate in a flat-bottomed bin: A comparison of the DEM model results with the experimental measurements,” *Powder Technology*, vol. 214, no. 3, pp. 322–336, Dec. 2011, doi: 10.1016/j.powtec.2011.08.042.
- [34] J. Horabik and M. Molenda, “Parameters and contact models for DEM simulations of agricultural granular materials: A review,” *Biosystems Engineering*, vol. 147, pp. 206–225, 2016, doi: <https://doi.org/10.1016/j.biosystemseng.2016.02.017>.
- [35] R. Kobyłka, M. Molenda, and J. Horabik, “DEM simulation of the pressure distribution and flow pattern in a model grain silo with an annular segment attached to the wall,” *Biosystems Engineering*, vol. 193, pp. 75–89, May 2020, doi: 10.1016/j.biosystemseng.2020.02.013.
- [36] S. Masson and J. Martinez, “Effect of particle mechanical properties on silo flow and stresses from distinct element simulations,” *Powder Technology*, vol. 109, no. 1–3, pp. 164–178, Apr. 2000, doi: 10.1016/S0032-5910(99)00234-X.
- [37] A. Ramírez, J. Nielsen, and F. Ayuga, “On the use of plate-type normal pressure cells in silos: Part 2: Validation for pressure measurements,” *Computers and Electronics in Agriculture*, vol. 71, no. 1, pp. 64–70, Apr. 2010, doi: 10.1016/j.compag.2009.12.005.
- [38] Y. Li, Y. Xu, and C. Thornton, “A comparison of discrete element simulations and experiments for ‘sandpiles’ composed of spherical particles,” *Powder Technology*, vol. 160, no. 3, pp. 219–228, Dec. 2005, doi: 10.1016/j.powtec.2005.09.002.
- [39] M. O. Ciantia, M. Arroyo, J. Butlanska, and A. Gens, “DEM modelling of cone penetration tests in a double-porosity crushable granular material,” *Computers and Geotechnics*, vol. 73, pp. 109–127, Mar. 2016, doi: 10.1016/j.compgeo.2015.12.001.
- [40] C. J. Coetzee, “Particle upscaling: Calibration and validation of the discrete element method,” *Powder Technology*, vol. 344, pp. 487–503, Feb. 2019, doi: 10.1016/j.powtec.2018.12.022.
- [41] S. Lommen, M. Mohajeri, G. Lodewijks, and D. Schott, “DEM particle upscaling for large-scale bulk handling equipment and material interaction,” *Powder Technology*, vol. 352, pp. 273–282, Jun. 2019, doi: 10.1016/j.powtec.2019.04.034.
- [42] M. J. Mohajeri, R. L. J. Helmons, C. van Rhee, and D. L. Schott, “A hybrid particle-geometric scaling approach for elasto-plastic adhesive DEM contact models,” *Powder Technology*, vol. 369, pp. 72–87, Jun. 2020, doi: 10.1016/j.powtec.2020.05.012.
- [43] D. S. Nasato, C. Goniva, S. Pirker, and C. Kloss, “Coarse Graining for Large-scale DEM Simulations of Particle Flow – An Investigation on Contact and Cohesion Models,” *Procedia Engineering*, vol. 102, pp. 1484–1490, 2015, doi: 10.1016/j.proeng.2015.01.282.
- [44] M. Sakai and S. Koshizuka, “Large-scale discrete element modeling in pneumatic conveying,” *Chemical Engineering Science*, p. 7, 2009.
- [45] S. C. Thakur, J. Y. Ooi, and H. Ahmadian, “Scaling of discrete element model parameters for cohesionless and cohesive solid,” *Powder Technology*, vol. 293, pp. 130–137, May 2016, doi: 10.1016/j.powtec.2015.05.051.
- [46] A. P. Grima and P. W. Wypych, “Development and validation of calibration methods for discrete element modelling,” *Granular Matter*, vol. 13, no. 2, pp. 127–132, Apr. 2011, doi: 10.1007/s10035-010-0197-4.

- [47] T. Roessler and A. Katterfeld, "Scaling of the angle of repose test and its influence on the calibration of DEM parameters using upscaled particles," *Powder Technology*, p. 9, 2018.
- [48] L. Xie, W. Zhong, H. Zhang, A. Yu, Y. Qian, and Y. Situ, "Wear process during granular flow transportation in conveyor transfer," *Powder Technology*, vol. 288, pp. 65–75, Jan. 2016, doi: 10.1016/j.powtec.2015.10.043.
- [49] F. Safranyik, "GRAVITATIONAL AND VIBRATIONAL DISCHARGE OF SILOS," SZENT ISTVÁN UNIVERSITY, Hungary, 2016.
- [50] I. Keppler, L. Kocsis, I. Oldal, I. Farkas, and A. Csatar, "Grain velocity distribution in a mixed flow dryer," *Advanced Powder Technology*, vol. 23, no. 6, pp. 824–832, Nov. 2012, doi: 10.1016/j.apt.2011.11.003.
- [51] EDEM, *EDEM 2018 Documentation*. Edinburgh, Scotland, UK: DEM Solutions Ltd, 2018.
- [52] A. Ramírez, J. Nielsen, and F. Ayuga, "Pressure measurements in steel silos with eccentric hoppers," *Powder Technology*, vol. 201, no. 1, pp. 7–20, Jul. 2010, doi: 10.1016/j.powtec.2010.02.027.
- [53] C. González-Montellano, E. Gallego, Á. Ramírez-Gómez, and F. Ayuga, "Three dimensional discrete element models for simulating the filling and emptying of silos: Analysis of numerical results," *Computers & Chemical Engineering*, vol. 40, pp. 22–32, May 2012, doi: 10.1016/j.compchemeng.2012.02.007.
- [54] C. González-Montellano, A. Ramírez, J. M. Fuentes, and F. Ayuga, "Numerical effects derived from en masse filling of agricultural silos in DEM simulations," *Computers and Electronics in Agriculture*, vol. 81, pp. 113–123, Feb. 2012, doi: 10.1016/j.compag.2011.11.013.
- [55] D. Markauskas, Á. Ramírez-Gómez, R. Kačianauskas, and E. Zdancevičius, "Maize grain shape approaches for DEM modelling," *Computers and Electronics in Agriculture*, vol. 118, pp. 247–258, Oct. 2015, doi: 10.1016/j.compag.2015.09.004.
- [56] J. Härtl, J. Y. Ooi, J. M. Rotter, M. Wojcik, S. Ding, and G. G. Enstad, "The influence of a cone-in-cone insert on flow pattern and wall pressure in a full-scale silo," *Chemical Engineering Research and Design*, vol. 86, no. 4, pp. 370–378, Apr. 2008, doi: 10.1016/j.cherd.2007.07.001.
- [57] A. Jenike and J. Johanson, "Bin loads," *J. Struct. Div.*, vol. 94, no. ST4, pp. 1011–1041, 1968.